

Photocatalytic degradation of the herbicide quinclorac in water using Mn (III) salen and solar light

Yisi YANG^{1,2,3}, Yan ZHANG^{2,3}, Qingru ZENG^{1,*}

¹College of Bioscience and Biotechnology, Hunan Agricultural University, Changsha, P.R. China

²Hubei Key Laboratory for Processing and Application of Catalytic Materials, College of Chemical Engineering, Huanggang Normal University, Huanggang, P.R. China

³College of Chemistry and Chemical Engineering, Huanggang Normal University, Huanggang, P.R. China

Received: 02.12.2016

Accepted/Published Online: 01.02.2018

Final Version: 01.06.2018

Abstract: Quinclorac (QNC) is a widely used herbicide and is persistent in surface and ground waters. Its residuals and converted products are hazardous to aquatic animals, vegetation, and microbes, and it is therefore important to degrade QNC using an efficient and environmental friendly technology. In this study, the photocatalytic degradation of QNC using [(R,R)-(N,N'-bis(3,5,3',5'-tetra-tert-butylsalicylidene)-1,2-cyclohexanediaminato] manganese(III) acetate (Mn (III) salen) and H₂O₂ was performed under natural sunlight irradiation and a 91% degradation rate was achieved in neutral pure water in 240 min. The identified degradation products confirmed that the cleavage of QNC molecules was the main process involved in the hydroxylation, along with the cracking of the N=C bond on the pyridine ring and hydroxylation on the benzoic ring. The active species analysis showed hydroxyl radicals and superoxide radicals were the main reactive species. Photocatalytic kinetics indicated that the degradation process was in accordance with a pseudo-first-order kinetic equation.

Key words: Photocatalytic degradation, quinclorac, sunlight, [(R,R)-(N,N'-bis(3,5,3',5'-tetra-tert-butylsalicylidene)-1,2-cyclohexanediaminato] manganese(III) acetate

1. Introduction

Quinclorac (3,7-dichloroquinoline-8-carboxylic acid: QNC), displayed in Figure 1, is a widely used auxin herbicide that can disturb the activity of hormonal regulation enzymes in herbs and then hinder their normal growth and metabolism. In China, it has been reported that excessive levels of QNC residues in tobacco fields have seriously prevented the growth of vegetation.^{1,2} It is also a concern that QNC residues in soil could be converted into potentially hazardous products or intermediates, which will endanger aquatic animals, vegetation, and microbes. When QNC residues enter surface and ground waters by rainfall leaching, they are resistant to hydrolysis and photolysis.^{3,4} Pan et al. reported that QNC inhibited the growth of submerged macrophytes in water.⁵ QNC has not been approved for agricultural use in Europe since 2008.⁴ In developing countries, there has not been such robust supervision on the use of QNC, with subsequent potential risks caused by its excessive use on farmland. As a consequence, QNC is the most frequently detected pesticide in lakes, where it is often present at $\mu\text{g/L}$ levels.^{6,7} To remediate QNC polluted water, studies had been conducted to assess the methods of biotransformation,⁸ photocatalysis^{4,9} and adsorption.^{10–12} Among them, photocatalysis is an excellent

*Correspondence: zqingru@126.com

green and environmentally friendly technology for the treatment of pollutant-contaminated water, in that it in situ induces active species to attack and oxidize the target compound to water, CO₂, and small molecules. Photocatalysts utilized for water decontamination can be classified into two groups: (a) semiconductors, and (b) organic compounds and metal organic complexes. In the presence of P25 TiO₂, QNC could be completely degraded in pure water in 40 min under the illumination of an 1100 W xenon lamp, but in paddy field water the irradiation time had to be extended to 130 min for complete degradation.⁴ Although P25 TiO₂ has excellent stability and optical performance, its absorption range is limited to the region of 320–400 nm, occupying only a small part of the total solar spectrum. Other semiconductor catalysts are intensively studied for the treatment of organic pollutant-contaminated water.^{13–15} While their typical drawbacks are that the major constituents of the normally used are rare noble metals, and most of semiconductors are susceptible to photocorrosion in aqueous solution, which causes the migration of metal ions into water.^{16,17} Thus, the adoption of expensive and rare materials would make the pollution remediation process not affordable from an economic point of view.

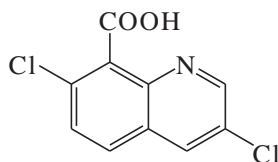
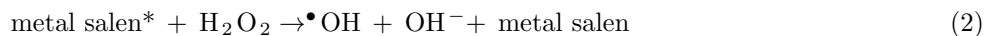
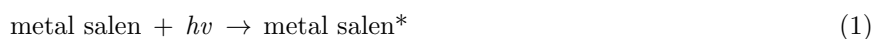


Figure 1. The structure of quinclorac (QNC).

Many organic dyes were employed as organic photocatalysts due to their absorption bands extending from UV to near infrared range.^{18–21} Some organic photocatalysts, such as porphyrins and phthalocyanines, can activate H₂O₂ or O₂ to produce reactive radicals, which are attractive approaches to organic pollutants degradation.^{22–24} Because of their solubility in water and potential harm to the ecoenvironment,^{25,26} many efforts have been dedicated to their immobilization onto supporters for recycling the organic photocatalysts for further use.^{27–29} Yet, in some cases, when compared with P25 TiO₂, these supported photocatalysts were similar or with even less photocatalytic efficiency for the oxidation of pollutants, the preparations of which were tedious.^{30–32} Metal salen are an ideal type of metal organic catalyst used for photodegradation of contaminants because of their high absorptivity in the UV-visible range. In addition, they are inexpensive, easily prepared, stable under light, and recyclable from water by filtration, which avoid the problems of other photocatalysts mentioned above.^{16,17} Metal salen are very capable of prompting the decomposition of H₂O₂ or O₂ to reactive radicals such as •OH, ¹O₂, and •O₂⁻.^{33,34} Therefore, they were utilized in the photodegradation of some organic dyes, such as rhodamine B (RhB), crystal violet, and malachite green, which could be efficiently degraded by [Fe(III) salen] and H₂O₂ under visible or UV light irradiation.^{35–37} Another study indicated that in the presence of an iron (III) Schiff base complex ¹O₂ was detected, and it played an important role in photodegrading RhB under visible light illumination.³⁸ With the photoassisted generation of reactive species, metal salen complexes have the potential to degrade organic pollutants in water:



Because most visible light photocatalytic experiments have been conducted under high power xenon lamps, not only is a lot of energy expended, but further mass applications are confined. Sunlight is available in sufficient quantities to drive photochemistry in most locations, and if sunlight can be utilized by more effective photocatalysts, the common drawback of the relatively high cost of xenon lamps and the electricity required could be overcome and the efficiency of photodegradation would be considerably improved.^{39,40}

To the best of our knowledge, there is no report regarding the application of metal salen and sunlight to produce active oxidant species that can decompose pesticides. The aim of the present study was to select an optimal metal salen complex to degrade QNC under irradiation from sunlight. First, the optimum experimental conditions and the dominant active species in the photodegradation process were determined. Then the degradation products of QNC were identified, and a plausible degradation mechanism of QNC in this system was proposed and discussed.

2. Results and discussion

2.1. Optimal photocatalyst

Four metal complexes and TiO₂ were applied to QNC solutions at identical concentrations of 50 mg/L, and were then irradiated by natural sunlight separately. As shown in Figure 2, complex c Mn (III) salen could effectively degrade QNC to 9% residual in 240 min. The Mn complex had a stronger catalytic activity than the Fe and Co complexes, which might be attributed to its strong absorption in the wide spectra wavelength range of solar light. In addition, the electronic effect of four tert-butyl groups on the salen ligand was beneficial for electron transfer from ligand to central metal, and then H₂O₂ would rapidly obtain electrons to form hydroxyl radicals and superoxide radicals. When no catalyst was present, there was little QNC degradation, even under the illumination of sunlight. In the presence of Mn (III) salen, the QNC degradation rate in the dark was still far less than that in sunlight. The pure P25 TiO₂ showed 31% degradation of QNC in 240 min. It was clear that it is critical for the catalyst to absorb energetic photons and produce active radicals to attack the target pollutant in this degradation process. For environmental considerations and to maximize the degradation effect, complex c Mn (III) salen was selected as the optimal catalyst for further studies.

2.2. Effect of the amount of catalyst

The effect of the amount of catalyst in the system was studied by varying the catalyst to substrate molar ratio in the range of 5%–20%, with the initial concentration of QNC held constant at 50 mg/L. As shown in Figure 3, after 240 min sunlight irradiation, the total degradation ratio was 47%, 54%, 89%, and 74% at catalyst to substrate molar ratios of 5%, 10%, 15%, and 20%, respectively. QNC degradation increased steadily when the amount of catalyst was increased until it reached 15%. At this point, a further increase in the amount of catalyst lowered the degradation rate. When the amount of catalyst was very high, the undissolved suspension would influence the penetration of light into the reactor, and the process efficiency would be impeded. Many previous studies have indicated that incident light into the reactor is a key factor that determines the optimal amount of catalyst.^{41,42} In addition, the aggregation of excess catalyst would limit the contact of QNC molecules with the catalyst.

Hence, to ensure the effective absorption of available photons and to save costs, the catalyst to substrate molar ratio was set at 15% as the optimal value for subsequent photodegradation experiments.

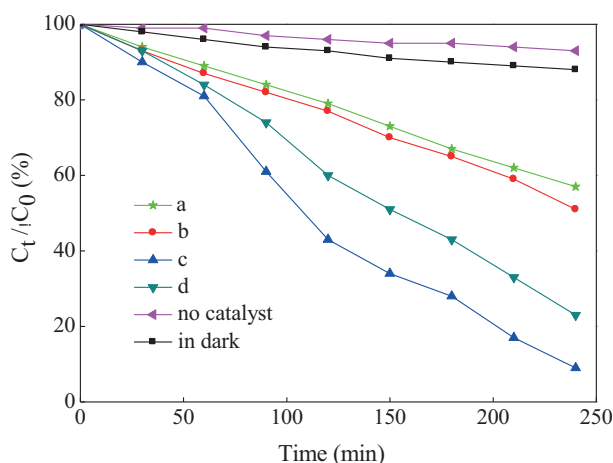


Figure 2. The effects of different catalysts on QNC degradation.

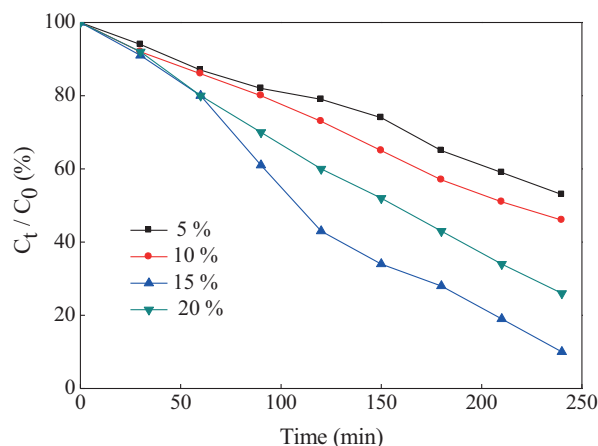


Figure 3. The effects of catalyst to substrate molar ratios on QNC degradation.

2.3. Effect of H₂O₂

As a cheap and temperate oxidant, H₂O₂ is commonly used in photodegradation reactions. Due to its electron accepting ability, it can react with electrons offered by a catalyst to generate hydroxyl radicals and superoxide radicals, which can then attack organic pollutants. As shown in Figure 4, the addition of H₂O₂ increased the degradation rate, but when the H₂O₂ concentration were too high (60 mg/L) or too low (20 mg/L), the effect would be lessened. The maximum degradation rate of 90% was achieved at an addition of 40 mg/L. Optimizing the ratio of H₂O₂ to QNC in this system would ensure hydroxyl radicals attacked QNC molecules easily. If the H₂O₂ concentration was higher than the optimal value, excess H₂O₂ would consume hydroxyl radicals through the reaction: H₂O₂ + •OH → H₂O + HO₂•. When the H₂O₂ concentration was less than optimal, there would not be sufficient •OH present in the system to attack the target pollutant.^{43,44} Therefore, the •OH concentration was affected by the amount of H₂O₂ available for photodegradation.

2.4. The role of active oxidant species in degradation

In photodegradation reactions, O₂, H₂O, and H₂O₂ are very important components that can generate active reactants such as •OH and •O₂⁻.^{45,46} To determine which was more crucial in QNC degradation, isopropanol (0.1 M) as an •OH scavenger was used to quench •OH as the important photo-induced species. Nitrogen was purged for 30 min to create anaerobic conditions and suppress the generation of •O₂⁻ from oxygen in the air, before adding H₂O₂ and catalyst. Benzoquinone (0.1 M) was added to quench •O₂⁻. A comparative experiment without quenchers and H₂O₂ was conducted under otherwise identical conditions. The pseudo-first-order kinetics curves obtained from these experiments are displayed in Figure 5. The lower rate constant of the degradation reaction when isopropanol was added indicated that hydroxyl radicals were important active oxidants in QNC decomposition. The degradation rate in the nitrogen atmosphere was close to that in the open atmosphere, which manifested that oxygen from the atmosphere had little influence on degradation. However, when there was no H₂O₂, the photodegradation reaction was clearly suppressed, even though no quenchers were added. Hence, in this system, the influence of oxygen from the atmosphere was negligible, and the contribution of •OH and •O₂⁻ was mainly determined by the amount of H₂O₂.

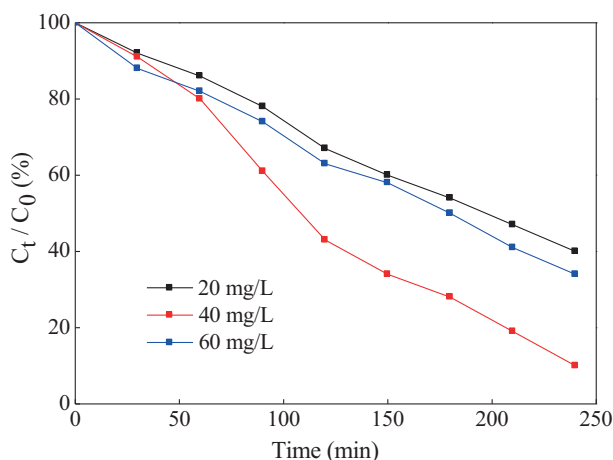


Figure 4. The effects of the amounts of H₂O₂ on QNC degradation.

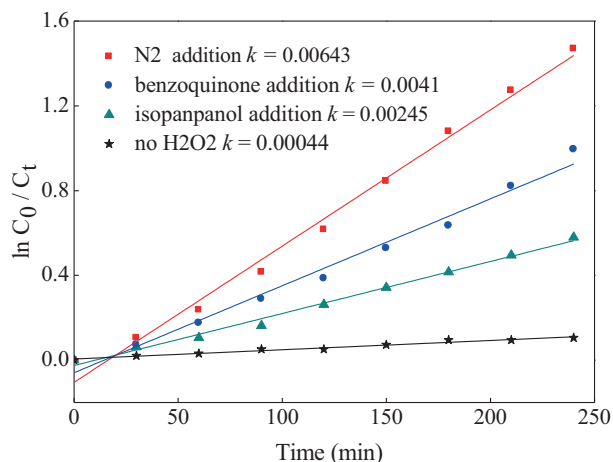


Figure 5. Pseudo-first-order kinetics of scavenger additions for QNC degradation.

2.5. Possible degradation mechanism

Three main products were detected by LC-MS. The main fragments ($M + 1$) and retention time for the three products are shown in Figure 6. Under illumination with sunlight, the photons could be absorbed by Mn (III) salen, then the shared electrons in the salen cycle could be transferred to the central metal and quickly captured by H₂O₂ to form active $\bullet\text{OH}$ and $\bullet\text{O}_2^-$ to attack organic pollutants near the catalyst. The attacks tended to take place at positions rich in electrons on the QNC molecules, such as the oxidative dechlorination and oxidative cleavage of the N=C bond on the pyridine ring, as well as hydroxylation on the benzoic ring. Hence, as shown in Figures 6 and 7, when three hydroxylated products were detected, two of them were due to cracking of bonds on the pyridine ring. The main degradation pathways of QNC in this system are thus: (1) dechlorination and cleavage of the N=C bond by $\bullet\text{OH}$ on the pyridine ring, (2) breakage of the double bond on the pyridine ring by $\bullet\text{O}_2^-$, and (3) hydroxylation of the benzene ring. Although some competition for $\bullet\text{OH}$ might exist between dechlorination and cleavage of the N=C bond on the pyridine ring, a previous study of the mechanism reported that a dechlorination and hydroxylation reaction in the C9 position, followed by opening of the pyridine ring, was the main degradation step for QNC photocatalytic treatment.⁴ The mechanism of QNC degradation in the system used in the present study was as described in Figure 7.

2.6. Recyclability of the catalyst

The stability of the Mn (III) salen catalyst was evaluated in four cyclic runs. For each run, a catalyst sample at a catalyst to substrate molar ratio of 15% was used for the photocatalytic degradation of QNC at 50 mg/L, under sunlight irradiation. The catalyst in each run was recovered with centrifugation and decantation, followed by overnight drying at 80 °C, with no further treatment. The results displayed in Figure 8 showed the stable performance of the catalysts, which were able to degrade 90%, 82%, 78%, and 74% of 50 mg/L of QNC in the four runs, respectively. A comparison between the IR spectrum of the fresh catalyst and of the catalysts recycled four times revealed almost no changes in the Mn (III) salen structure.

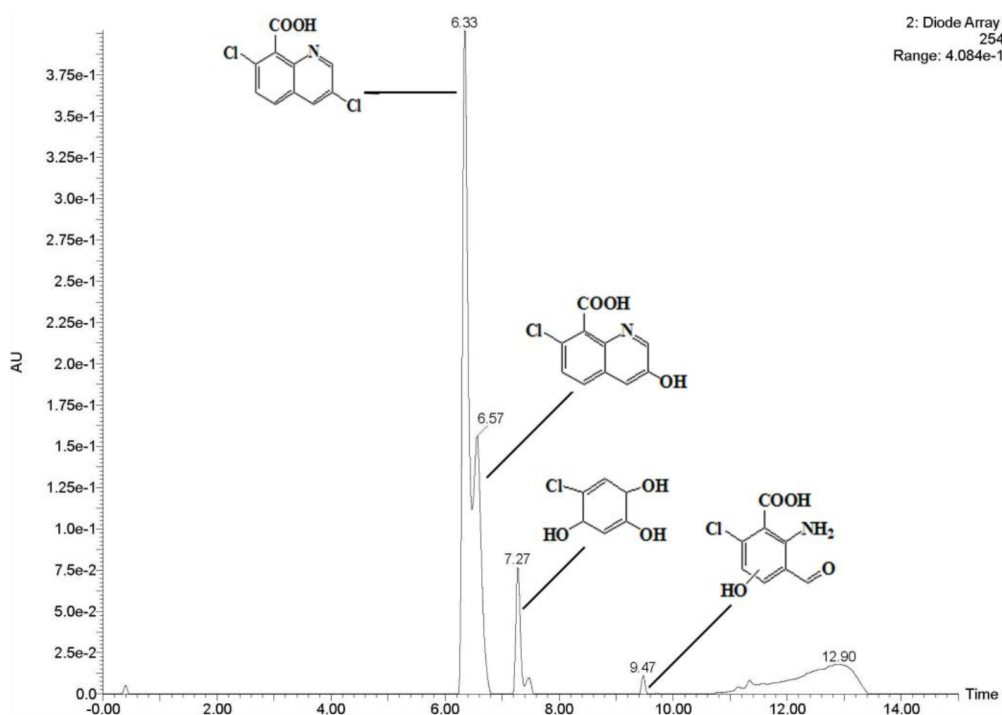


Figure 6. The high performance liquid chromatography (HPLC) spectra of QNC photocatalytic products.

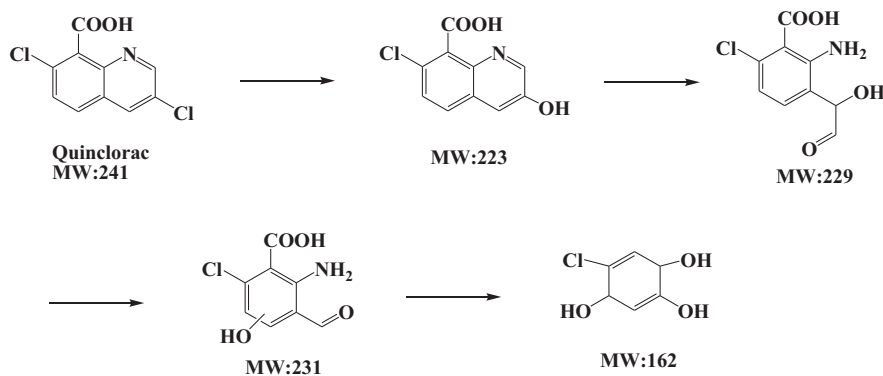


Figure 7. The posited mechanism of QNC photocatalytic degradation.

3. Experimental

3.1. Chemicals

All aqueous solutions were prepared with ultrapure water ($>18.2 \text{ M}\Omega\cdot\text{cm}$) from a Milli-Q Plus system (Millipore, TU-1900, Beijing Purkinje General Instrument Co., Ltd., Beijing, China). A 98% pure QNC standard was supplied by Jiangsu Biological Pesticide Ltd (Jiangsu, China). All other reagents were analytical grade and were purchased from Sigma-Aldrich. TiO_2 is Degussa P25 TiO_2 . Metal salen catalysts were synthesized according to the literature and characterized using an infrared spectrometer.

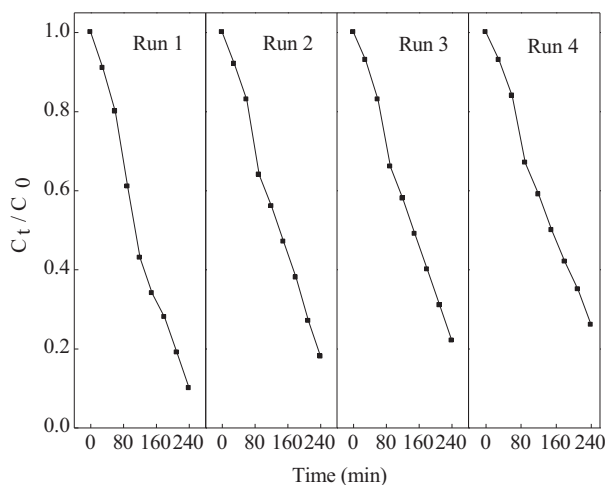


Figure 8. Four recycling runs of Mn (III) salen for QNC photocatalytic degradation.

3.2. Synthesis procedures and characterization

The photocatalysts were synthesized according to a published method.^{47,48} (1) Synthesis of salen ligand. In a 50 mL round-bottom flask, 1 mmol of cyclohexane diamine was dissolved in 1 mL of anhydrous ethanol, by stirring for 12 min. A mixed solution of 2 mmol of salicylaldehyde and 10 mL of anhydrous ethanol was added to the flask, heated at reflux for 2 h, and then cooled to room temperature. The yellow precipitates (salen ligand) that formed were then filtered and washed with cold ethanol. The salen ligand was dried overnight in a vacuum oven at 70 °C. To increase catalytic efficiency, tert-butyl as an electron-donating group was introduced into C3, C3', C5, and C5' on the salen ligand (ditertbutylsalicylaldehyde replaced salicylaldehyde). (2) Synthesis of Mn-Salen. In a 150 mL round bottom flask, 1.5 mmol of manganese acetate and an equivalent amount of the salen ligand were mixed in 20 mL of ethanol and heated to reflux in argon. Then 0.4 mL of glacial acetic acid was added to the solution at room temperature, which was stirred together with a supply of oxygen overnight. Finally, the manganese complex was precipitated by adding diethyl ether to the reaction mixture, and the product was isolated, washed, and crystallized from acetone to obtain pure Mn-Salen. For other metal complexes shown in Figure 9, Fe and Co were used as the core metals to coordinate with salen ligands using this procedure.

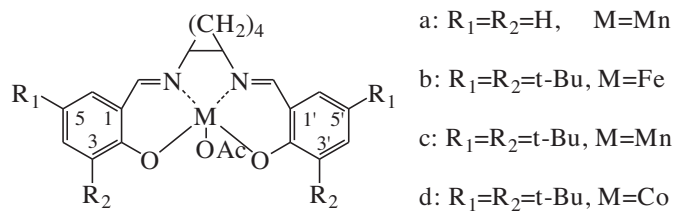


Figure 9. The structures of four metal salen complexes.

Four different metal salen complexes were analyzed using infrared spectroscopy and are described as follows: ligand. IR (KBr, cm^{-1}) ν_{max} : 2973, 2865, 1626, 1475. a. IR (KBr, cm^{-1}) ν_{max} : 2937, 2865, 1636, 1540. b. IR (KBr, cm^{-1}) ν_{max} : 2964, 2862, 1540, 1607. c. IR (KBr, cm^{-1}) ν_{max} : 2969, 2912, 1612, 1636. d. IR (KBr, cm^{-1}) ν_{max} : 2975, 2856, 1525, 1598. The characteristic absorption peaks were in accordance with previously reported peaks.⁴⁷⁻⁴⁹

The optical properties of four metal salen complexes and a salen ligand were measured by UV-Vis spectrophotometer (UV-2600, Shimadzu, Tokyo, Japan) equipped with an integrating sphere attachment, and a UV-Vis Thermo Evolution 300 spectrophotometer (Thermo Fisher Scientific, Waltham, MA, USA). The spectral analysis showed that all samples had strong absorption at ~ 338 , ~ 322 , and ~ 259 nm, as displayed in Figure 10, which were assigned to ligand $n-\pi^*$ and $\pi-\pi^*$ charge transfer bands. All metal salen complexes exhibited a broader band centered around 500–600 nm, which was ascribed to a ligand-to-metal charge transfer band. Compared to the other three catalysts, complex c had a wider absorption band in the range of 200–700 nm and above, and therefore the strong photonic energy in this region can be absorbed sufficiently to prompt the transfer of ligand electrons to Mn, which were then captured by H_2O_2 to induce active radicals. Therefore, Mn (III) salen was applicable for use as a UV-visible light active photocatalyst.

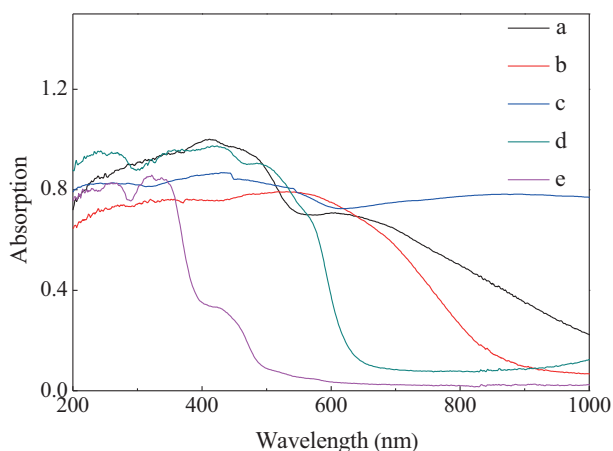


Figure 10. UV-Vis absorption spectra of metal salen complexes a, b, c, d, and e (ligand).

3.3. Degradation experiment

To optimize the use of natural solar light, degradation experiments were performed at 114.87°E, 30.44°N, from 10:30 to 14:30 on sunny days in May. The temperature was approximately 25 ± 2 °C. In a 250 mL glass beaker (diameter: 7.1 cm and height 9.7 cm), 100 mL of 50 mg/L QNC solution containing a catalyst (the molar ratio of catalyst to QNC was set to 15%) and H_2O_2 (40 mg/L) was irradiated by sunlight for 240 min. All experiments were repeated three times and average values of data were calculated to ensure accuracy. The reaction solution was magnetically stirred at 180 rpm. At every designated time interval, 5 mL of solution in photocatalytic reaction was taken out and centrifuged, and the supernatants were analyzed with high performance liquid chromatography (HPLC) and the degradation products were detected by liquid chromatography-mass spectrometry (LC-MS).

3.4. Chemical analysis

The QNC concentration and transformed products were monitored by Agilent 1200 HPLC system (Agilent, USA) and an Agilent 1100 series LC/MSD Mass Trap Spectrometer (Agilent Technologies, UK). The chromatographic system was equipped with a diode array detector and an Agilent (Santa Clara, CA, USA) C18 column (50 mm \times 2.1 mm \times 1.7 μm). The column temperature was maintained at 30 °C during the analysis. The mobile phase A was methanol, while the mobile phase B was 0.1% glacial acetic acid in water, and the

proportion of A in the eluent increased from 5% A (0 min) to 95% (10 min), before being kept at 95% for 2 min; it then increased to 100% for 1 min, at which point it decreased to 5%, where it was maintained for 2 min. The flow rate was set at 0.5 mL/min and the injection volume was 10 μ L. The detection wavelength was set at 254 nm. Under these conditions, the retention time of QNC was 6.33 min. Molecular fragments were generated using an electrospray ion source. The particular operational conditions were as follows: ion-source temperature = 400 °C, nitrogen was used as the drying and nebulizer gas, high-purity nitrogen was used as the collision gas, and ion-spray voltage floating = 4500. The mass range monitored was 100–1000 Da.

4. Conclusions

Because of its wide range of absorption from the ultraviolet to near infrared spectrum, [(R,R)-(N,N-bis(3,5,3',5'-tetra-tert-butylsalicylidene)-1,2-cyclohexanediaminato] manganese(III) acetate is a robust photocatalyst that can fully utilize solar energy to decontaminate refractory herbicides. The photodegradation and dechlorination of QNC were observed in the presence of Mn (III) salen under sunlight irradiation. The main products detected after degradation confirmed that the cleavage of QNC molecules involves hydroxylation along with cracking of the N=C bond on the pyridine ring and hydroxylation on the benzoic ring. Active oxidant species such as \bullet OH and \bullet O₂⁻ were mainly derived from H₂O₂ decomposition, which was photocatalyzed by Mn (III) salen. Furthermore, this photocatalytic system is both energy-efficient and environmentally friendly, due to the application of natural sunlight and a recyclable cheap catalyst.

Acknowledgment

This work was supported by the Educational Commission of Hubei Province of China (B2016205).

References

- Han, J.; Zhang, Z.; Liu, H.; Wang, X. Q. *Acta. Tabacaria Sin.* **2013**, *19*, 81-83.
- Liu, H. S.; Jing-Xin, L. I.; Han, J. F.; Shu-Xia, X. U.; Zuo, T.; Yuan, S. H. *Acta Agriculturae Boreali-Sinica* **2010**, *25*, 156-158.
- Pinna, M. V.; Pusino, A. *Chemosphere* **2011**, *86*, 655-658.
- Pareja, L.; Pérezparada, A.; Agüera, A.; Cesio, V.; Heinzen, H.; Fernándezalba, A. R. *Chemosphere* **2012**, *87*, 838-844.
- Pan, H. Y.; Li, X. L.; Xu, X. H.; Gao, S. X. *J. Environ. Sci.* **2009**, *21*, 307-312.
- Pareja, L.; Martínez-Bueno, M. J.; Cesio, V.; Heinzen, H.; Fernández-Alba, A. R. *J. Chromatogr. A* **2011**, *1218*, 4790-4798.
- Mattice, J. D.; Skulman, B. W.; Norman, R. J.; Gbur, E. E. *J. Soil Water Conserv.* **2010**, *65*, 130-140.
- Li, Z. M.; Shao, T. J.; Min, H.; Lu, Z. M.; Xu, X. Y.; *Soil Biol. Biochem.* **2009**, *41*, 984-990.
- Pinna, M. V.; Pusino, A. *Chemosphere* **2011**, *86*, 655-658.
- Pusino, A.; Gelsomino, A.; Fiori, M. G.; Gessa, C. *Clays Clay Miner.* **2003**, *51*, 143-149.
- Ding, C.; Gong, D.; Yu, P.; Shao, J.; Zhong, M. *Desalin. Water Treat.* **2016**, *57*, 1-12.
- Mekhloufi, M.; Zehhaf, A.; Benyoucef, A.; Quijada, C.; Morallon, E. *Environ. Monit. Assess.* **2013**, *185*, 10365-10375.
- Wang, H.; Zhang, L.; Chen, Z.; Hu, J.; Li, S.; Wang, Z.; Liu, J.; Wang, X. *Chem. Soc. Rev.* **2014**, *43*, 5234-5244.
- Gondal, M. A.; Sayeed, M. N.; Alarfaj, A. *Chem. Phys. Lett.* **2007**, *445*, 325-330.

15. Liu, S. Q. *Environ. Chem. Lett.* **2012**, *10*, 209-216.
16. Wang, C. C.; Li, J. R.; Lv, X. L.; Zhang, Y. Q.; Guo, G. *Energy Environ. Sci.* **2014**, *7*, 2831-2867.
17. Fresno, F.; Portela, R.; Suarez, S.; Coronado, J. M. *J. Mater. Chem. A* **2014**, *2*, 2863-2884.
18. Dinçalp, H.; İçli, S. *Sol. Energy* **2006**, *80*, 332-346.
19. Cho, Y. M.; Choi, W. Y.; Lee, C. H.; Hyeon, T.; Lee, H. I. *Environ. Sci. Technol.* **2001**, *35*, 966-970.
20. Chu, W.; Chan, K. H.; Jafvert, C. T.; Chan, Y. S. *Chemosphere* **2007**, *69*, 177-183.
21. Sanjuan, A.; Aguirre, G.; Alvaro, M.; Garcia, H.; Scaiano, J. C. *Appl. Catal. B-Environ.* **2000**, *25*, 257-265.
22. Silva, M.; Calvete, M. J. F.; Gonçalves, N. P. F.; Burrows, H. D.; Sarakha, M.; Fernandes, A. *J. Hazard. Mater.* **2012**, *233-234*, 79-88.
23. Silva, M.; Azenha, M. E.; Pereira, M. M.; Burrows, H. D.; Sarakha, M.; Forano, C.; Ribeiro, M. F.; Fernandes, A. *Appl. Catal. B-Environ.* **2010**, *100*, 1-9.
24. Sorokin, A.B.; Tuel, A. *Catal. Today* **2000**, *57*, 45-59.
25. Tsai, W. T.; Hsu, H. C.; Su, T. Y.; Lin, K. Y.; Lin, C. M.; Dai, T. H. *J. Hazard. Mater.* **2007**, *147*, 1056-1062.
26. Wang, C.; Zhang, J.; Wang, P.; Wang, H.; Yan, H. *Desalin. Water Treat.* **2013**, *53*, 3681-3690.
27. Bonesi, S. M.; Carbonell, E.; Garcia, H.; Fagnoni, M.; Albin, A. *Appl. Catal. B-Environ.* **2008**, *79*, 368-376.
28. Miranda, M. A.; Amat, A. M.; Arques, A. *Catal. Today* **2002**, *76*, 113-119.
29. Aprile, C.; Maret, L.; Alvaro, M.; Scaiano, J. C.; Garcia, H. *Dalton Trans.* **2008**, *40*, 5465-5470.
30. Sanjuan, A.; Alvaro, M.; Aguirre, G.; Garcia, H.; Scaiano, J. C. *J. Am. Chem. Soc.* **1998**, *120*, 7351-7352.
31. Alvaro, M.; Carbonell, E.; Garcia, H.; Lamaza, C.; Pillai, M. N. *Photochem. Photobiol. Sci.* **2004**, *3*, 189-193.
32. Bayarri, B.; Carbonell, E.; Gimenez, J.; Esplugas, S.; Garcia, H. *Chemosphere* **2008**, *72*, 67-74.
33. Oszajca, M.; Brindell, M.; Łukasz Orzeł; Dąbrowski, J. M.; Śpiewak, K.; Łabuz, P.; Pacia, M.; Stochel-Gaudyn, A.; Macyk, W.; Eldik, R.; et al. *Coordin. Chem. Rev.* **2016**, *327-328*, 143-165.
34. Iranzo, O. *Bioorg. Chem.* **2011**, *39*, 73-87.
35. Gazi, S.; Ananthkrishnan, R.; Singh, N. D. P. *J. Hazard. Mater.* **2010**, *183*, 894-901.
36. Wu, Q.; Hao, X.; Feng, X.; Wang, Y.; Li, Y.; Wang, E.; Zhu, X.; Pan, X. *Inorg. Chem. Commun.* **2012**, *22*, 137-140.
37. Meng, X.; Qin, C.; Wang, X. L.; Su, Z. M.; Li, B.; Yang, Q. H. *Dalton. Trans.* **2011**, *40*, 9964-9966.
38. Song, Q.; Ma, W. H.; Jia, M. K.; Johnson, D.; Huang, Y. P. *Appl. Catal. A-Gen.* **2015**, *505*, 70-76.
39. Souza, B. M.; Dezotti, M. W. C.; Rui, A. R. B.; Vilar, V. J. P. *Chem. Eng. J.* **2014**, *256*, 448-457.
40. Prieto-Rodríguez, L.; Spasiano, D.; Oller, I.; Fernández-Calderero, I.; Agüera, A.; Malato, S. *Catal. Today* **2013**, *209*, 188-194.
41. Herrmann, J. *Top. Catal.* **2005**, *34*, 49-65.
42. Cassano, A. E.; Alfano, O. E. *Catal. Today* **2000**, *58*, 167-197.
43. Hayat, K.; Gondal, M. A.; Khaled, M. M.; Ahmed, S. *Mol. Catal. A-Chem.* **2011**, *336*, 64-71.
44. Monteagudo, J. M.; Durán, A.; Aguirre, M.; Martín, I. S. *Chem. Eng. J.* **2010**, *162*, 702-709.
45. Chong, M. N.; Jin, B.; Chow, C. W. K.; Saint, C. *Water Res.* **2010**, *44*, 2997-3027.
46. Bai, C.; Xiao, W.; Feng, D.; Xian, M.; Guo, D.; Ge, Z.; Zhou, T. S. *Chem. Eng. J.* **2013**, *215-216*, 227-234.
47. Larrow, J. F.; Jacobsen, E. N.; *J. Org. Chem.* **1994**, *59*, 1939-1942.
48. Jacobsen, E. N.; Zhang, W.; Muci, A. R.; Ecker, J. R.; Deng, L. *J. Am. Chem. Soc.* **1991**, *113*, 7063-7064.
49. Johansson, M.; Purse, B. W.; Terasaki, O.; Bäckvall, J. E. *Adv. Synth. Catal.* **2008**, *350*, 1807-1815.